Australian Government
Department of Defence
Defence Science and
Technology Organisation

Calculation of Radar Probability of Detection in K-Distributed Sea Clutter and Noise

Stephen Bocquet

Joint Operations Division
Defence Science and Technology Organisation

DSTO-TN-1000

ABSTRACT

The detection performance of maritime radars is usually limited by sea clutter. The K distribution is a well established statistical model of sea clutter which is widely used in performance calculations. There is no closed form solution for the probability of detection in K-distributed clutter, so numerical methods are required. The K distribution is a compound model which consists of Gaussian speckle modulated by a slowly varying mean level, this local mean being gamma distributed. A series solution for the probability of detection in Gaussian noise is integrated over the gamma distribution for the local clutter power. Gauss-Laguerre quadrature is used for the integration, with the nodes and weights calculated using matrix methods, so that a general purpose numerical integration routine is not required. The method is implemented in Matlab and compared with an approximate solution based on lookup tables. The solution described here is slower, but more accurate and more flexible in that it allows for a wider range of target fluctuation models.

RELEASE LIMITATION

Approved for public release

Published by

Joint Operations Division
DSTO Defence Science and Technology Organisation
Fairbairn Business Park Department of Defence
Canberra ACT 2600 Australia

Telephone: (02) 6265 9111
Fax: (02) 6265 2741

AR 014-977
April 2011

APPROVED FOR PUBLIC RELEASE

Calculation of Radar Probability of Detection in K-Distributed Sea Clutter and Noise

Executive Summary

Modelling of the radar returns from the sea is required for operations analysis of maritime patrol, in order to calculate probabilities of detection for targets of interest. The detection performance of maritime radars is usually limited by sea clutter. A statistical model of the clutter is normally used, and the K distribution has become standard for this purpose. There is no closed form solution for the probability of detection in K-distributed clutter, so numerical methods are required. A method for calculation of the probability of detection in K-distributed clutter and noise is described, and compared with other approaches. It is faster than direct numerical integration, and more flexible and more accurate, but slower, than an approximate method based on interpolation. Faster evaluation is highly desirable for simulation models used in operations research. The method described here could be used to create tables for interpolation, which should produce the appropriate mix of speed and accuracy for operations research simulation models.

Contents

1. Introduction

Modelling of the radar returns from the sea is required for operations analysis of maritime patrol, in order to calculate probabilities of detection for targets of interest. In this context the backscatter from the sea is referred to as sea clutter. A statistical model of the clutter is normally used, and the K distribution has become standard for this purpose [1]. Sea clutter consists of a rapidly varying speckle component and an underlying mean amplitude which varies more slowly. The K distribution provides a compound representation which includes both components. Thermal noise, which has Gaussian statistics, must also be considered in calculating probabilities of detection. Fluctuations in the target return also need to be taken into account, and this is normally done with statistical models based on the gamma distribution.

The calculation of the probability of detection in K-distributed clutter and noise is quite difficult. An approximate method was developed by Watts and Wicks [2,3]. This method is fast, because the probability of detection is obtained by linear interpolation in a table, following some preliminary calculations which need only be done once for each set of parameters. However, the result is only approximate, and the necessary tables of coefficients [3] are only available for the Swerling 1 and 2 target fluctuation models, as well as a non-fluctuating target (Swerling 0). Alternatively, the probability of detection can be calculated by numerical integration over the K distribution. This will give accurate results, but it is slow, and therefore impractical for use in simulations where the probability of detection must be updated frequently. Another approach is described in [1], and further explored in this report, in which the K distribution is separated into its components and only the integration over the local clutter power is carried out numerically.

2. Probability of Detection

2.1 The K Distribution

The K distribution for the clutter intensity can be expressed as

$$P(z) = \int_0^\infty P(z \mid x) P_c(x) dx \tag{1}$$

where

$$P(z \mid x) = \frac{1}{x} \exp(-z/x) \tag{2}$$

and

$$P_c(x) = \frac{b^\nu x^{\nu-1}}{\Gamma(\nu)} \exp(-bx) \tag{3}$$

Equation (3) is the Gamma distribution for the local clutter power x. The mean power is

$$p_c = \langle x \rangle = \nu / b \tag{4}$$

Equation (1) evaluates to

$$P(z) = \frac{2b}{\Gamma(\nu)} \left(\sqrt{bz} \right)^{\nu-1} K_{\nu-1} \left(2\sqrt{bz} \right) \tag{5}$$

The modified Bessel function K in equation (5) gives the distribution its name. However, for calculating the probability of detection it is advantageous to keep the speckle and modulation components separate, assuming that the local clutter power x remains constant over the beam dwell time.

2.2 Probability of Detection Calculation

The probability of detection in Gaussian noise and speckle is

$$P_d(Y \mid x, N) = \int_Y^\infty P_R(\mu \mid s, N)\, d\mu \tag{6}$$

The threshold Y is normalised by the noise and local clutter power x.

The sum of N radar returns, normalised by the noise and local clutter power is

$$\mu = \frac{1}{x + p_n} \sum_{i=1}^{N} z_i \tag{7}$$

The sum of the target powers from the N pulses is

$$s = \frac{1}{x + p_n} \sum_{i=1}^{N} A_i^2 \tag{8}$$

The probability density function for the sum μ of N radar returns from a fixed target in Gaussian noise is the multilook Rice distribution,

$$\begin{aligned} P_R(\mu \mid s, N) &= \left(\frac{\mu}{s} \right)^{(N-1)/2} e^{-(\mu+s)} I_{N-1} \left(2\sqrt{\mu s} \right) \\ &= \sum_{i=0}^{\infty} \frac{e^{-\mu} \mu^{N+i-1}}{(N+i-1)!} \frac{e^{-s} s^i}{i!} \end{aligned} \tag{9}$$

The series form of equation (9) is obtained using the series expansion for the Bessel function [4, §8.445]:

$$I_n(z) = \sum_{i=0}^{\infty} \frac{1}{i! \Gamma(n+i+1)} \left(\frac{z}{2} \right)^{n+2i} \tag{10}$$

The integral in equation (6) can be evaluated to give the double sum formula for the probability of detection for a fixed target [5,6,7]:

$$\begin{aligned}\int_Y^\infty P_R(\mu \mid s,N)d\mu &= \sum_{i=0}^{\infty}\frac{e^{-s}s^i}{i!}\frac{1}{(N+i-1)!}\int_Y^\infty e^{-\mu}\mu^{N+i-1}d\mu \\ &= \sum_{i=0}^{\infty}\frac{e^{-s}s^i}{i!}e^{-Y}\sum_{j=0}^{N+i-1}\frac{Y^j}{j!} \\ &= \sum_{i=0}^{\infty}\frac{e^{-s}s^i}{i!}e^{-Y}\left(\sum_{j=0}^{N-1}\frac{Y^j}{j!}+\sum_{j=N}^{N+i-1}\frac{Y^j}{j!}\right) \\ &= \sum_{j=0}^{N-1}e^{-Y}\frac{Y^j}{j!} \quad + \quad \sum_{i=0}^{\infty}\frac{e^{-s}s^i}{i!}\sum_{j=N}^{N+i-1}e^{-Y}\frac{Y^j}{j!} \\ &= \sum_{j=0}^{N-1}e^{-Y}\frac{Y^j}{j!} \quad + \quad \sum_{j=N}^{\infty}e^{-Y}\frac{Y^j}{j!}\left(1-\sum_{i=0}^{j-N}\frac{e^{-s}s^i}{i!}\right)\end{aligned} \tag{11}$$

The manipulation of the series in equation (11) makes use of the result

$$\sum_{i=0}^{\infty}\frac{e^{-s}s^i}{i!}=1 \tag{12}$$

Target fluctuations are modelled using the Gamma distribution for the sum of target returns s:

$$P_T(s \mid S,k)=\frac{s^{k-1}}{\Gamma(k)}\left(\frac{k}{S}\right)^k e^{-ks/S} \tag{13}$$

where

$$S=\frac{N\left\langle A^2\right\rangle}{x+p_n} \tag{14}$$

The Gamma distribution encompasses all the Marcum-Swerling and Weinstock target models [8],[9, Section B] as shown in the table below:

Weinstock	0 < k < 1
Swerling 1	k = 1
Swerling 2	k = N
Swerling 3	k = 2
Swerling 4	k = 2N
Swerling 0	k → ∞

A non-fluctuating target (Swerling 0) corresponds to k → ∞ or s = S.

The probability of detection for a fluctuating target is [9, Section B]

$$\begin{aligned} P_d(Y \mid x,S,k,N) &= \int_0^\infty P_T(s \mid S,k) \int_Y^\infty P_R(\mu \mid s,N)\, d\mu\, ds \\ &= \sum_{j=0}^{N-1} e^{-Y} \frac{Y^j}{j!} \quad + \quad \sum_{j=N}^{\infty} e^{-Y} \frac{Y^j}{j!} \left(1 - \sum_{i=0}^{j-N} \frac{1}{\Gamma(k) i!} \left(\frac{k}{S} \right)^k \int_0^\infty e^{-s(1+k/S)} s^{i+k-1} ds \right) \quad (15) \\ &= \sum_{j=0}^{N-1} e^{-Y} \frac{Y^j}{j!} \quad + \quad \sum_{j=N}^{\infty} e^{-Y} \frac{Y^j}{j!} \left(1 - \sum_{i=0}^{j-N} \frac{\Gamma(k+i)}{\Gamma(k) i!} \left(\frac{k}{S+k} \right)^k \left(\frac{S}{S+k} \right)^i \right) \end{aligned}$$

Numerical calculation of the probability of detection from equations (11) and (15) is not straightforward, due to underflow and loss of significance. Appendix A gives some insight into the nature of the series in these equations, and shows why it is not always possible to begin the summation with the first term, even with high precision arithmetic. Shnidman [5,6,7,9,10] has developed methods to carry out these calculations efficiently, and coded the resulting algorithms in Matlab [1]. Chernoff bounds (Appendix B) are used to avoid unnecessary calculations.

2.3 Integration over the Clutter Power

The probability of detection in K-distributed clutter with a single pulse threshold y_n and local clutter power x is

$$P_d(y_n, N) = \int_0^\infty P_d(Y \mid x, N) P_c(x) dx \quad (16)$$

where $P_d(Y \mid x)$ is calculated as for detection in noise, equation (6), and $P_c(x)$ is the Gamma distribution (3). The threshold y_n is normalised by the sum of the noise power p_n and the mean clutter power p_c. At first sight, numerical integration over the local clutter power seems unlikely to provide a fast and efficient method for calculating the probability of detection. However, if we make the substitution $t = bx$ in the Gamma distribution (3) this becomes

$$P_c(x)dx = P_c(t)dt = \frac{t^{\nu-1} e^{-t}}{\Gamma(\nu)} dt \quad (17)$$

In terms of the mean clutter power p_c, $t = \nu x / p_c$. Equation (16) becomes

$$P_d(y_n, N) = \frac{1}{\Gamma(\nu)} \int_0^\infty P_d(Y \mid t, N) t^{\nu-1} e^{-t} dt \quad (18)$$

This integral is readily evaluated using Gauss-Laguerre quadrature [11, Section 4.5]. The Laguerre polynomials are generated from a recurrence relation, and the nodes and weights are calculated from the eigenvalues and eigenvectors of a symmetric tridiagonal matrix. Gautschi [12] has written Matlab code to do this. In most cases sufficient accuracy in P_d is

[1] Private communication.

obtained with only 10 quadrature points. The exception is low thresholds and $\nu < 1$, where many more points are needed to cope with the singularity at the origin. However, this situation is not of much practical importance, because a high threshold is needed to achieve a satisfactory probability of false alarm when ν is small. The maximum value of ν for which this method of integration can be used in Matlab is 171, because it requires $\Gamma(\nu)$ to be less than the largest floating point number which can be represented, i.e. $\Gamma(\nu) < 10^{308}$. As $\nu \to \infty$ the clutter becomes noise like, so integration over the Gamma distribution is not required. There is a very small, but perceptible, difference between the probability of detection calculated for $\nu = 170$ and the Rayleigh limit where the clutter is treated as noise.

2.4 Normalisation

The threshold Y is normalised by the noise and local clutter power. In terms of a single pulse, unnormalised threshold y

$$Y = \frac{Ny}{x + p_n} \tag{19}$$

We would like to express this in terms of the clutter to noise ratio CNR and the integration variable t.

$$\begin{aligned} Y &= \frac{y}{p_c + p_n} \frac{N(p_c + p_n)}{\frac{t\,p_c}{\nu} + p_n} \\ &= y_n \frac{N(1+CNR)}{1+\frac{t}{\nu}CNR} \end{aligned} \tag{20}$$

where y_n is the single pulse threshold normalised by the mean clutter plus noise power.

In the same way we would like to express the signal S in terms of the signal to noise ratio SNR, the clutter to noise ratio CNR and the integration variable t. From equation (14),

$$\begin{aligned} S &= \frac{N\left\langle A^2 \right\rangle}{x + p_n} \\ &= \frac{N\left\langle A^2 \right\rangle}{\frac{t\,p_c}{\nu} + p_n} \\ &= \frac{N\ SNR}{1+\frac{t}{\nu}CNR} \end{aligned} \tag{21}$$

For the clutter only case we have $p_n = 0$ or $CNR \to \infty$ so

$$Y = y_n \frac{N\nu}{t} \quad \text{and} \quad S = \frac{N\nu}{t} SCR \tag{22}$$

where SCR is the signal to clutter ratio.

2.5 Probability of False Alarm

The probability of false alarm is obtained from equation (11) with s = 0 (note that $0^0 \equiv 1$)

$$P_{fa}(Y \mid x, N) = \sum_{j=0}^{N-1} e^{-Y} \frac{Y^j}{j!} = \frac{\Gamma(N, Y)}{\Gamma(N)} \tag{23}$$

In terms of the Matlab incomplete gamma function, P_{fa} = 1 – gammainc(Y,N).

In order to calculate the probability of detection for a given probability of false alarm, the threshold must be determined from the probability of false alarm. This can be done using the Matlab root finding function fzero. This function requires either a starting estimate for the root, or an interval which brackets the root. In the first case fzero searches for the starting interval itself, which tends to cause it to fail, because the probability of false alarm is undefined for negative thresholds, and underflows to zero for large positive thresholds. A starting interval of 0.1 to 1100 for y_n was found to be satisfactory. Integration over the local clutter power does not impede the calculation much, because the nodes and weights depend only on ν, so they don't need to be recalculated during the root finding process.

In the case of a single pulse return from clutter, the integral over the clutter power can be evaluated to give

$$\begin{aligned} P_{fa}(y_n) &= \frac{1}{\Gamma(\nu)} \int_0^\infty P_{fa}(Y \mid t, 1) t^{\nu-1} e^{-t} dt \\ &= \frac{2(\nu y_n)^{\nu/2}}{\Gamma(\nu)} K_\nu \left(2\sqrt{\nu y_n} \right) \end{aligned} \tag{24}$$

This solution is used in Section 3.4 to assess the accuracy of the numerical integration with different numbers of quadrature points.

3. Sample Calculations

3.1 Probability of False Alarm

Figure 1 shows the probability of false alarm for a single pulse return from K-distributed clutter, for different values of the shape parameter ν. Figure 1 reproduces Figure 8.6 from reference [1].

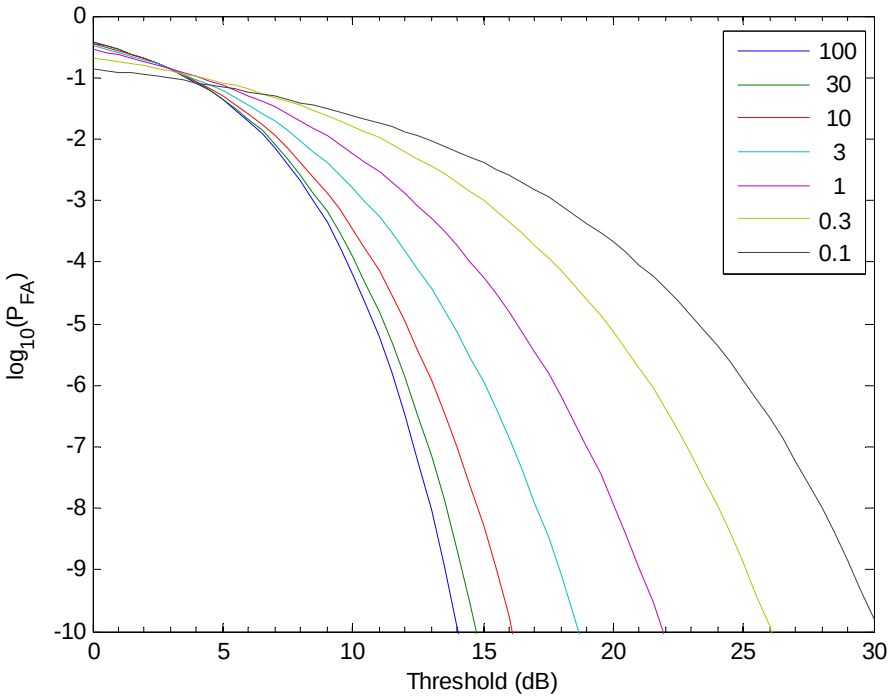

Figure 1 Probability of false alarm for a single pulse return from K-distributed clutter, for different values of the shape parameter ν

3.2 Probability of Detection

Figure 2 shows the probability of detection for a single pulse return from a fixed target in K-distributed clutter with ν = 10, for different probabilities of false alarm. Figure 2 reproduces the top graph in Figure 8.11 from reference [1]. Figure 3 shows the probability of detection for the incoherent sum of 10 pulses from a Swerling 1 target in K-distributed clutter with ν = 0.1, for different probabilities of false alarm. Figure 3 reproduces the bottom graph in Figure 8.14 from reference [1].

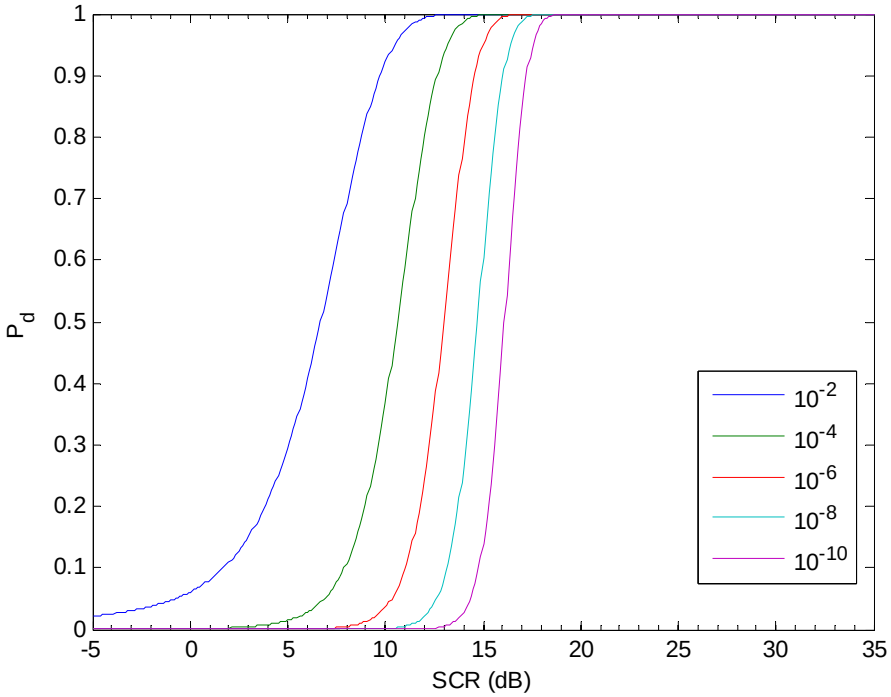

Figure 2 Probability of detection for a single pulse return from a fixed target in K-distributed clutter with $\nu = 10$, for different probabilities of false alarm

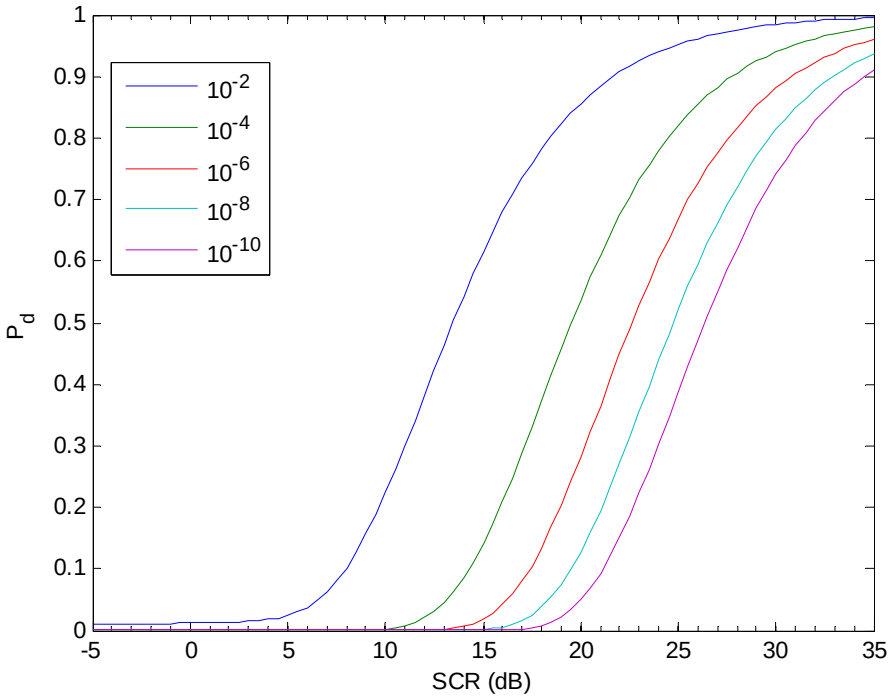

Figure 3 Probability of detection for the incoherent sum of 10 pulses from a Swerling 1 target in K-distributed clutter with $\nu = 0.1$, for different probabilities of false alarm

3.3 Target Fluctuation Models

Figure 4 shows the probability of detection for the Swerling target models in noise following incoherent integration of 16 pulses. Figure 4 reproduces the top graph in Figure 8.17 from reference [1].

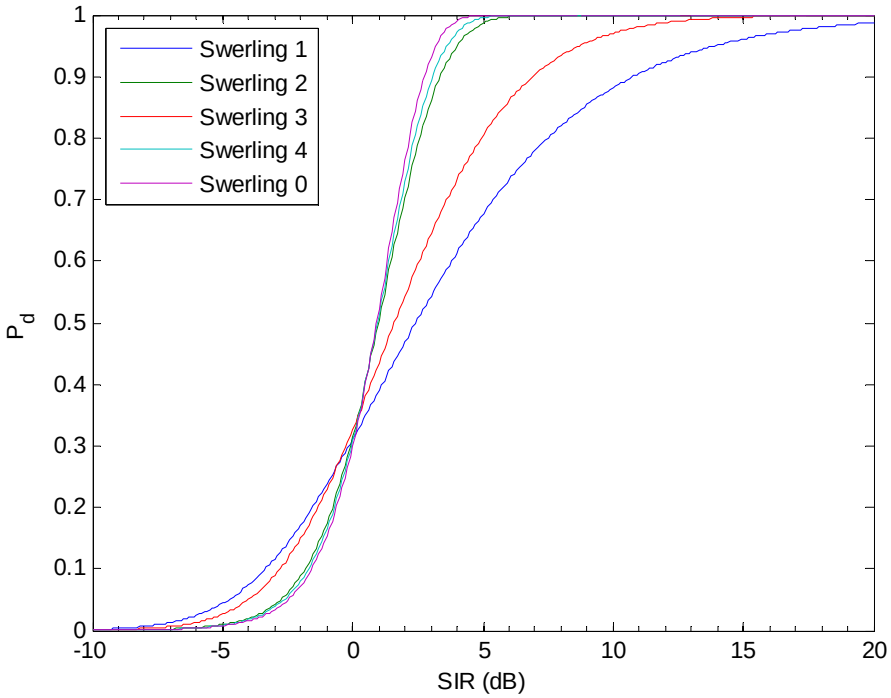

Figure 4 Probability of detection for Swerling target models in noise following incoherent integration of 16 pulses, with a probability of false alarm of 10^{-4}

3.4 Convergence of the Integral over the Clutter Power

Gaussian quadrature with n points is exact for an integrand in the form of a polynomial of order 2n [11, Section 4.5]. The integrand here is not a simple polynomial, so the number of quadrature points required for a sufficiently accurate result needs to be established. Figure 5 shows the probability of false alarm for a single pulse return from K-distributed clutter with $\nu = 0.1$, for different numbers of quadrature points, along with the analytic solution. Figure 6 shows the relative error in the probability of false alarm in Figure 5. It is noticeable that the number of points required to reduce the relative error to a satisfactory level is greater for low thresholds. Figure 7 shows the probability of detection for a single pulse return from a Swerling 2 target in K-distributed clutter with $\nu = 0.1$ and a probability of false alarm of 10^{-2}, calculated with different numbers of quadrature points. Figure 8 shows the absolute error in the probability of detection in Figure 7, estimated as the difference between the P_d for the set number of quadrature points and that using 150 points. The absolute error with 10 quadrature points is less than 10^{-2} for all signal to clutter ratios.

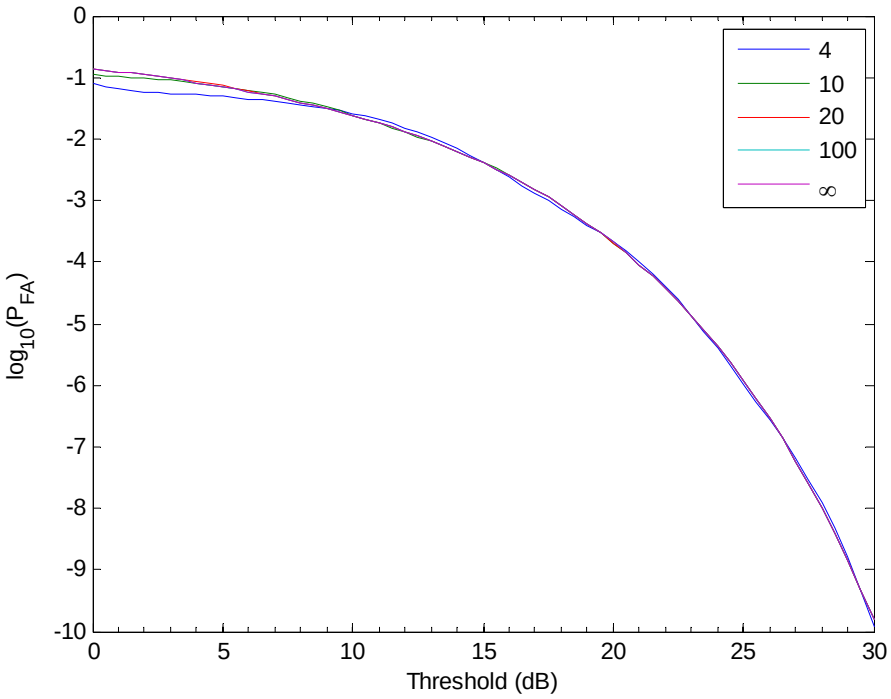

Figure 5 Probability of false alarm for a single pulse return from K-distributed clutter with ν = 0.1, for different numbers of quadrature points. The infinite limit is the analytic solution, equation (24).

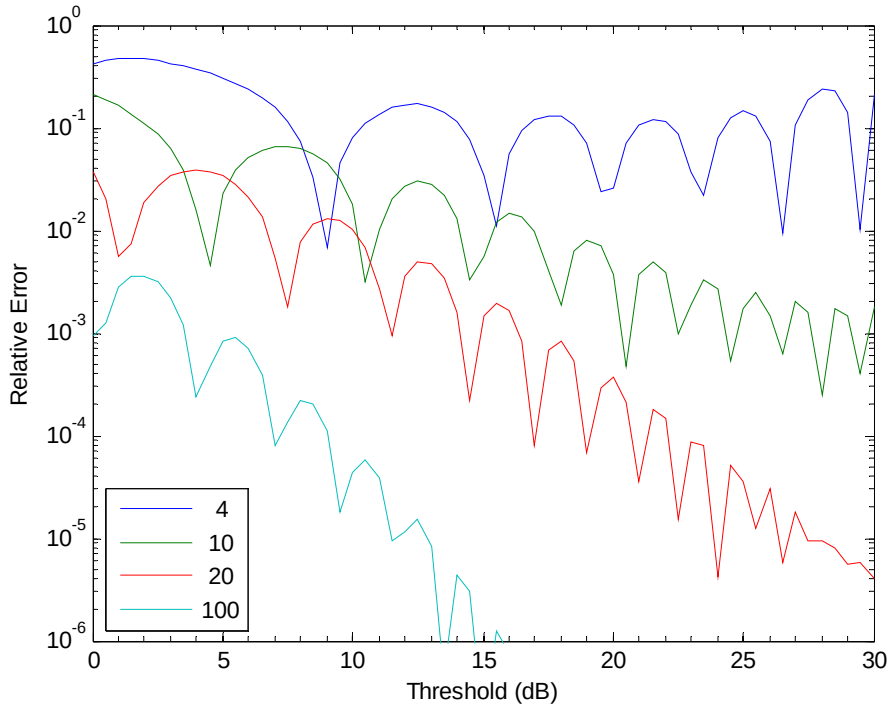

Figure 6 Relative error in the probability of false alarm in Figure 5

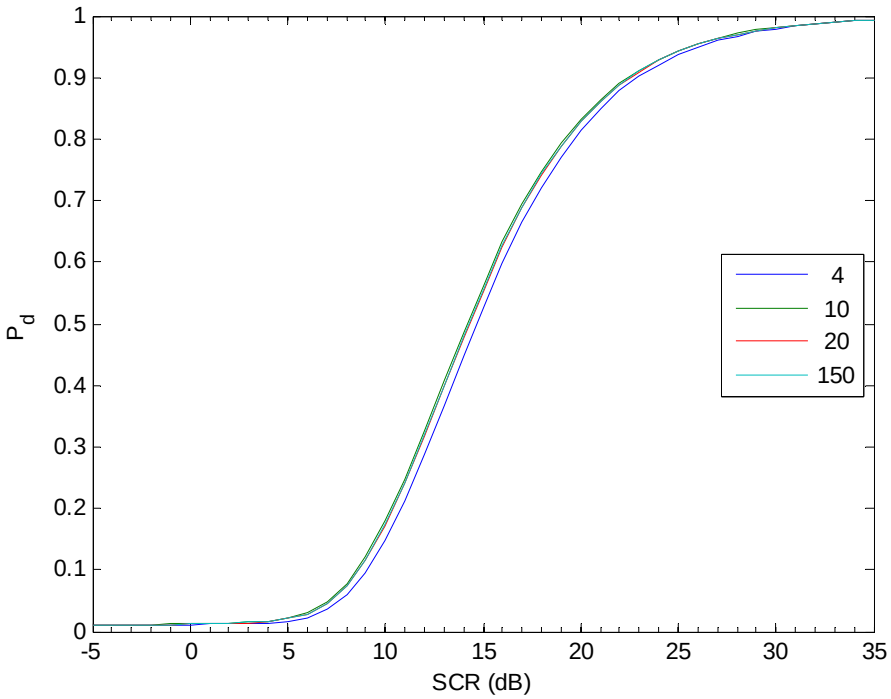

Figure 7 Probability of detection for a single pulse return from a Swerling 2 target in K-distributed clutter with $\nu = 0.1$ and a probability of false alarm of 10^{-2}, calculated with different numbers of quadrature points

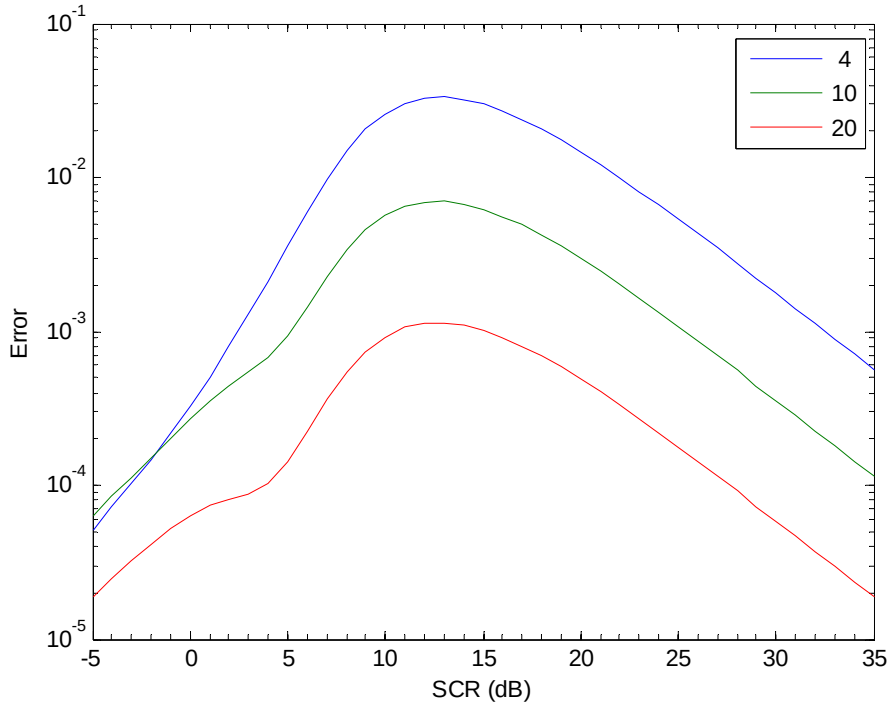

Figure 8 Absolute error in the probability of detection in Figure 7

3.5 Rayleigh Limit

Figure 9 shows the probability of detection for the incoherent sum of 10 pulses from a Swerling 2 target in K-distributed clutter, for different values of the clutter shape parameter ν. As noted in Section 2.3, the largest value of ν for which the integration over the clutter power can be done in Matlab is 171. Figure 9 shows this is not quite the same as the Rayleigh limit of $\nu \to \infty$ where the clutter can be treated as noise.

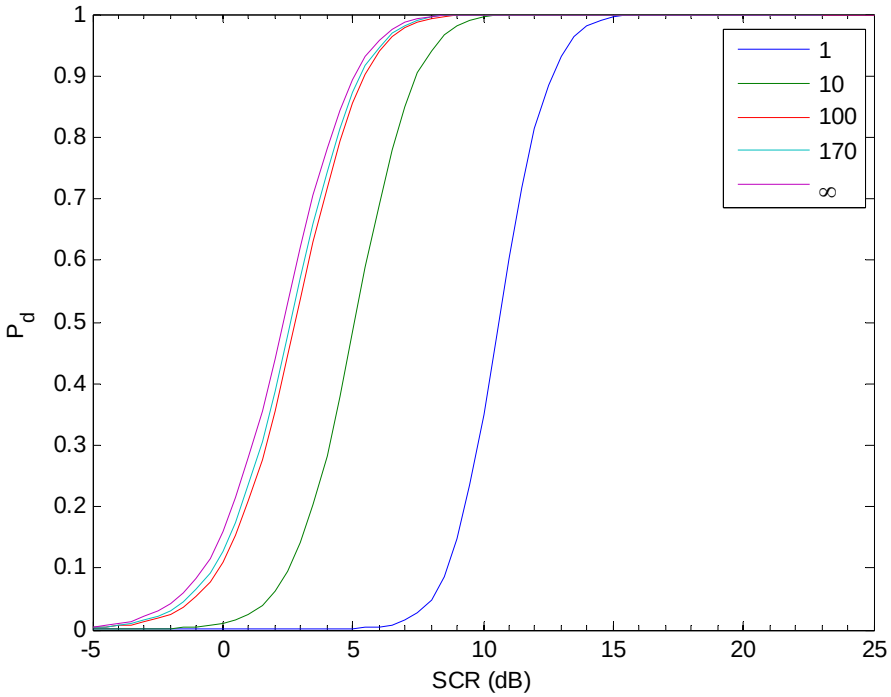

Figure 9 Probability of detection for the incoherent sum of 10 pulses from a Swerling 2 target in K-distributed clutter, for different values of the clutter shape parameter ν and a probability of false alarm of 10^{-4}

3.6 Comparison with the Method of Watts and Wicks

Figure 10 shows the probability of detection for the incoherent sum of 5 pulses from a Swerling 2 target in K-distributed clutter, for different values of the clutter shape parameter ν. Figure 10 reproduces Figure 6 from reference [3]. Calculation of 182 data points in Matlab required 0.11 s using the method of Section 2 (the curves in Figure 10) and 0.04 s using the method of Watts and Wicks [2,3] (dots in Figure 10) [2]. The speed comparison is quite favourable because the nodes and weights for the numerical integration only need to be calculated once for each curve in Figure 10. In a simulation model the clutter shape parameter will normally be different for each data point, so the nodes and weights must be recalculated every time. In this situation the method described here is slower than the method of Watts

[2] Calculations carried out with Matlab R2009b on a 32 bit desktop computer with a 3.2 GHz dual core Pentium processor, running Windows XP.

and Wicks by a factor of about 30. The method of Watts and Wicks is an approximation which involves only linear interpolation in a table, following some preliminary calculations. The method described here is slower, but more accurate and more flexible in that it allows a wider range of target fluctuation models with no additional work. The coefficients required for the method of Watts and Wicks have only been published for Swerling 0, 1 and 2 targets [3]; calculation of the necessary coefficients for other target models would be quite laborious.

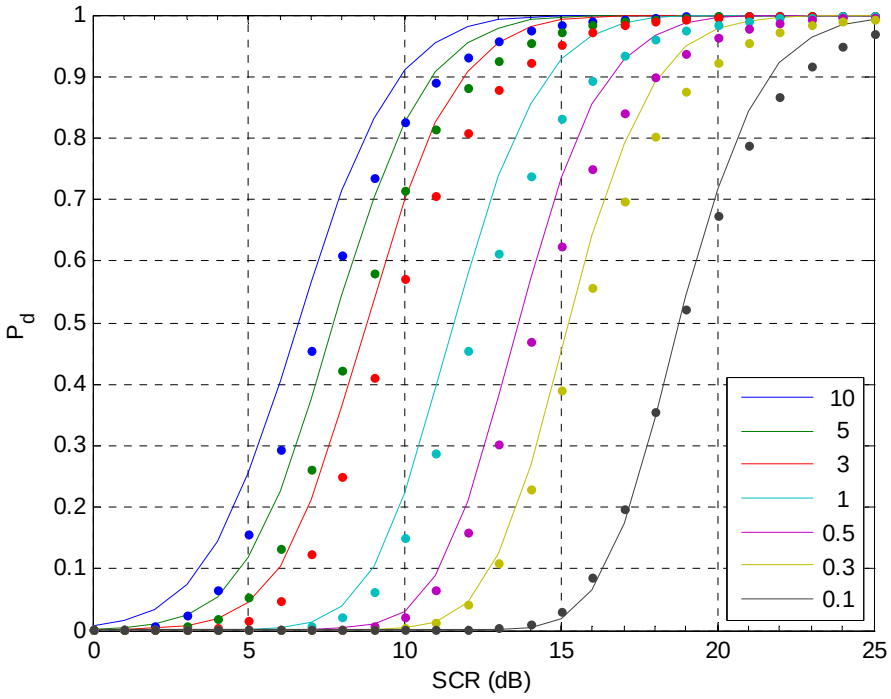

Figure 10 Probability of detection for the incoherent sum of 5 pulses from a Swerling 2 target in K-distributed clutter, for different values of the clutter shape parameter ν and a probability of false alarm of 10^{-4}. The curves are calculated using the method described in Section 2, and the dots are calculated using the method of Watts and Wicks [2,3].

3.7 Interpolation Scheme

Faster evaluation is highly desirable for simulation models used in operations research. The method of calculation described here could be used to create interpolation tables for P_d, which may assist in speeding up computation in some situations. A possible interpolation scheme is explored in Appendix C.

4. Possible Extensions

4.1 Constant False Alarm Rate Processing

Constant false alarm rate (CFAR) processing is often used to adapt the detection threshold to the changing clutter background. A variety of schemes are used [1, Chapter 9], some more amenable to mathematical analysis than others. The limiting case is 'ideal CFAR' in which the threshold follows the clutter background exactly. Ideal CFAR can be modelled by adapting the calculations described above, but the resulting probability of detection is unrealistically high, particularly for spiky clutter (small ν) [1, Section 9.2.3.7]. The fixed threshold calculation is more useful for operations analysis because it gives an estimate of worst case performance. Another approach is to calculate the detection performance for a fixed threshold and then apply a separately calculated CFAR loss [1]. Shnidman [9] has devised mathematical expressions for cell averaging CFAR, but these are based on a non-central chi-square distribution for the clutter [13] instead of the K distribution.

4.2 KK Distribution

The KK distribution is a linear combination of two K distributions with different parameters, used when non-Rayleigh white caps or sea spikes extend the tail of the distribution [14,15]. It should be straightforward to extend the method of calculation described here to the KK distribution, simply by replacing equation (1) with the sum of two integrals, one for each component of the distribution.

4.3 Clutter Correlations

The method described by Ward, Tough and Watts [1] allows for pulse to pulse correlation in the clutter speckle with an effective number of looks L which is less than N, the number of pulses integrated. In the case of fixed frequency operation, where the clutter speckle is constant from pulse to pulse, $L = 1$. Military radars generally use frequency agility to decorrelate the clutter from pulse to pulse. Residual correlation in the clutter can be accounted for with the effective number of looks $L < N$, with L not necessarily an integer [16]. The basic framework of the calculation is similar, but the clutter speckle is included with the target fluctuations instead of adding it to the noise. The integration over the local clutter power remains the same, but the probability of detection in equations (11) and (15) is replaced with more complicated expressions [1, Chapter 8] [3].

4.4 Target Models

Shnidman [17] has further expanded on the Swerling target models by including a persistent component in the target reflection, which is modelled using either the non-central gamma or the non-central gamma-gamma distribution. These expanded models are intended for targets

[3] The author has coded these expressions in Matlab, and reproduced Figures 8.7, 8.15 and 8.16 from [1], but the code is rather slow and inefficient. It is not clear if (or how) the method can be applied in the clutter only case, when the noise power is zero.

where the Swerling cases do not work well for high signal to noise ratios, and the Weibull or log-normal distributions have previously been used to model the signal fluctuations. In operations analysis we are mainly concerned with finding the performance limit for low signal to interference ratios, and the target models provided by the gamma distribution should be sufficient for this.

5. Conclusion

A method for calculation of the probability of detection in K-distributed clutter and noise has been described. The probability of detection in the local clutter power plus noise is obtained from a series solution, and this solution is integrated over the gamma distribution for the local clutter power. The method is faster than direct numerical integration over the K distribution, and it may be suitable for use in simulation models for operations research. It is slower, but more flexible and more accurate, than the method of Watts and Wicks, an approximate method based on interpolation. Faster evaluation is highly desirable for simulation models used in operations research. The method described here could be used to create tables for interpolation, which should produce the appropriate mix of speed and accuracy for operations research simulation models.

6. Acknowledgements

Josef Zuk provided the reference to the work of Gautschi [12] on orthogonal polynomials for Gaussian quadrature. Doug Driscoll coded the method of Watts and Wicks [2,3] in Matlab. Thanks to Luke Rosenberg and Yunhan Dong for their comments and corrections to the draft of this report.

7. References

1. K.D. Ward, R.J.A. Tough and S. Watts, *Sea Clutter: Scattering, the K Distribution and Radar Performance*, The Institution of Engineering and Technology, London (2006).

2. S. Watts and D.C. Wicks, *Empirical models for detection prediction in K-distribution radar sea clutter*, IEEE International Radar Conference (1990).

3. S. Watts, *A practical approach to the prediction and assessment of radar performance in sea clutter*, IEEE International Radar Conference (1995).

4. I.S. Gradshteyn and I.M. Ryzhik, *Table of integrals, series and products*, 5th edition, Academic Press (1994).

5. D.A. Shnidman, *Efficient Evaluation of the Probabilities of Detection and the Generalized Q-Function*, IEEE Trans. Inform. Theory **22** (1976) 746-751.

6. D.A. Shnidman, *The Calculation of the Probability of Detection and the Generalized Marcum Q-Function*, IEEE Trans. Inform. Theory **35** (1989) 389-400.

7. D.A. Shnidman, *Note on "The Calculation of the Probability of Detection and the Generalized Marcum Q-Function"*, IEEE Trans. Inform. Theory **37** (1991) 1233.

8. P. Swerling, *Recent Developments in Target Models for Radar Detection Analysis*, AGARD Conference Proceedings **66** Advanced Radar Systems, Istanbul, Turkey (1970).

9. D.A. Shnidman, *Radar Detection Probabilities and their Calculation*, IEEE Trans. AES **31** (1995) 928-950.

10. D.A. Shnidman, *Update on Radar Detection Probabilities and their Calculation*, IEEE Trans. AES **44** (2008) 380-383.

11. W.H. Press, S.A. Teukolsky, W.T. Vetterling and B.P. Flannery, *Numerical Recipes in Fortran*, Second Edition, Cambridge University Press (1992).

12. W. Gautschi, *Orthogonal Polynomials (in Matlab)*, J. Comp. App. Math. **178** (2005) 215-234.

13. D.A. Shnidman, *Generalized Radar Clutter Model*, IEEE Trans. AES **35** (1999) 857-865.

14. Y. Dong, *Distribution of X-Band High Resolution and High Grazing Angle Sea Clutter*, DSTO-RR-0316 (2006).

15. L. Rosenberg, D.J. Crisp and N.J. Stacy, *Analysis of the KK-distribution with medium grazing angle sea-clutter,* IET Radar Sonar Navig., **4** (2010) 209-222.

16. Y. Dong, *Distribution of Multi-Look Correlated K-Distributed Data*, Progress in Radar Research, Adelaide (2010).

17. D.A. Shnidman, *Expanded Swerling Target Models*, IEEE Trans. AES **39** (2003) 1059-1069.

18. G. Arfken, *Mathematical Methods for Physicists*, Second Edition, Academic Press, New York (1970).

19. M. Sankaran, *Approximations to the non-central chi-square distribution*, Biometrika **50** (1963) 199-204.

20. J.M. Wozencraft and I.M. Jacobs, *Principles of Communications Engineering*, Wiley, New York (1965).

21. S. Watts, *Radar Detection Prediction in K-Distributed Sea Clutter and Thermal Noise*, IEEE Trans. AES **23** (1987) 40-45.

22. S. Bocquet, *Analysis of Maritime Patrol and Response Missions*, DSTO-TR-2346 (2009).

Appendix A: The Series Expansion for the Probability of Detection in Noise

Some insight into the nature of the series for the probability of detection in noise can be gained using the Stirling approximation for the gamma function [18, equation (7.141)]:

$$\begin{aligned} \Gamma(z) = (z-1)! = \frac{z!}{z} \approx z^z e^{-z}\sqrt{\frac{2\pi}{z}} \\ \text{or} \quad \ln\Gamma(z) \approx z\ln z - z + \tfrac{1}{2}\ln(2\pi) - \tfrac{1}{2}\ln(z) \end{aligned} \tag{25}$$

The terms in the first sum from equations (11) and (15) are in the form

$$p_m = \frac{Y^m e^{-Y}}{m!} = \frac{Y^m e^{-Y}}{m\Gamma(m)} \tag{26}$$

Hence

$$\begin{aligned} \ln p_m &\approx m\ln Y - Y - \ln m - m\ln m + m - \tfrac{1}{2}\ln(2\pi) + \tfrac{1}{2}\ln(m) \\ &= m\ln\left(\frac{Y}{m}\right) - Y + m - \tfrac{1}{2}\ln(2\pi m) \\ &\approx m\left(\frac{Y}{m} - 1 - \tfrac{1}{2}\left(\frac{Y}{m}-1\right)^2\right) - Y + m - \tfrac{1}{2}\ln(2\pi m) \\ &= -\tfrac{1}{2m}\left(Y-m\right)^2 - \tfrac{1}{2}\ln(2\pi m) \end{aligned} \tag{27}$$

and

$$p_m \approx \frac{\exp\left(-\frac{1}{2m}\left(Y-m\right)^2\right)}{\sqrt{2\pi m}} \tag{28}$$

so for large Y the series terms form a normal distribution with mean Y and variance m. It follows that the number of terms required to obtain a desired accuracy in P_d is proportional to the square root of Y, and the required terms are centred around $m = Y$. If Y is large the terms are very small for small m, so it is not possible to start the series evaluation at $m = 0$, because the first term will underflow to zero. The approximation (28) is only valid for large Y and m. The problem of finding a suitable starting value for m is addressed by Shnidman [6] using the approximation

$$p_m \approx \frac{1}{\sqrt{2\pi}}\exp\left(-u^2\right) \quad \text{where} \quad u = \sqrt{2Y - \left(m - \tfrac{1}{2}\right)} - \sqrt{m - \tfrac{1}{2}} \tag{29}$$

which is valid for $m < 2Y$ and $m >> ½$. This is derived from an approximation for the non-central chi-square distribution [19].

Appendix B: Chernoff Bounds

If the precision of the computer arithmetic is ε, P_d evaluates to 1 for $P_d > 1 - \varepsilon$. Similarly, P_d evaluates to zero for $P_d < \varepsilon_m$, where ε_m is the smallest number which can be represented on the computer. For the double precision arithmetic in Matlab, $\varepsilon \sim 10^{-15}$ and $\varepsilon_m \sim 10^{-308}$. Chernoff bounds [9, Section IV B],[20] provide a means to avoid unnecessary calculations in these cases. We use ε for the lower bound and $1 - \varepsilon$ for the upper bound.

The unit step function can be bounded from above by $\exp(\lambda(x-t))$, and from below by $1 - \exp(-\lambda(x-t))$, for positive λ (Figure 11).

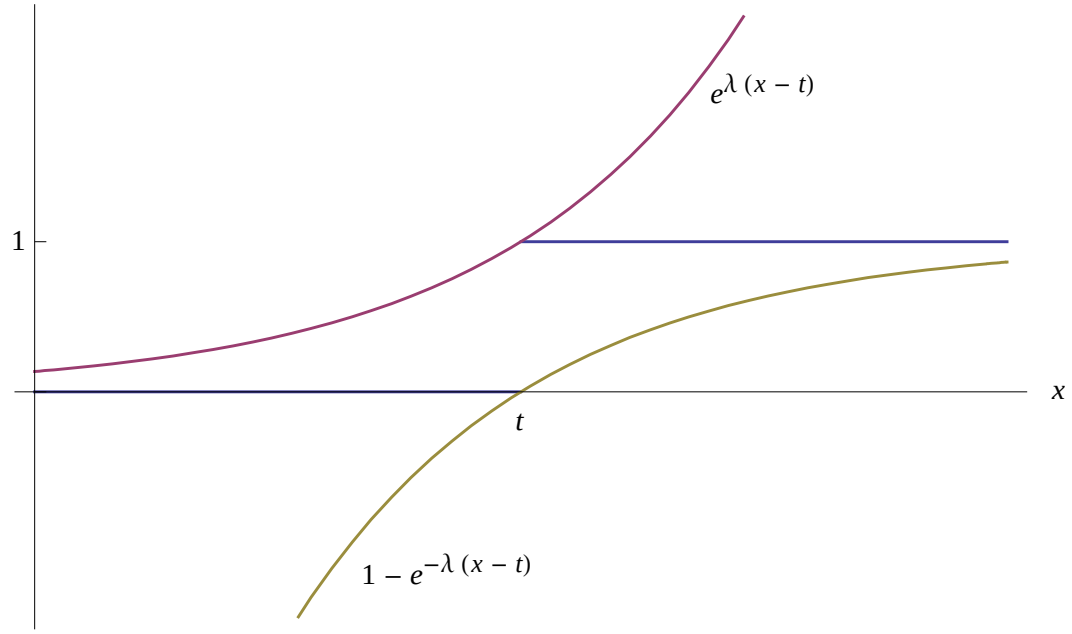

Figure 11 Upper and lower bounds to the unit step function

Since

$$\int_t^\infty f(x)dx = \int_0^\infty u(x-t) f(x)dx \tag{30}$$

we can bound this integral from above or below by replacing the unit step function with the appropriate bound. These bounds are generally easier to evaluate than the original integral, and the parameter λ can be chosen to give the closest bound.

From equations (6) and (9), the probability of detection for N radar returns from a fixed target in noise is

$$P_d(N,s,Y) = \int_Y^\infty \left(\frac{\mu}{s}\right)^{(N-1)/2} e^{-(\mu+s)} I_{N-1}\left(2\sqrt{\mu s}\right) d\mu. \tag{31}$$

The Chernoff bound for this case is

$$\begin{aligned} C_B(N,s,Y,\lambda) &= \int_0^\infty e^{\lambda(\mu-Y)}\left(\frac{\mu}{s}\right)^{(N-1)/2} e^{-(\mu+s)} I_{N-1}\left(2\sqrt{\mu s}\right) d\mu \\ &= \frac{\exp(-\lambda Y + Ns\lambda/(1-\lambda))}{(1-\lambda)^N}. \end{aligned} \tag{32}$$

The value of λ which gives the closest bound is obtained by solving

$$\frac{d\ln(C_B)}{d\lambda} = -Y + \frac{Ns}{(1-\lambda)^2} + \frac{N}{1-\lambda} = 0 \tag{33}$$

for λ. Equation (33) can be rearranged to form a quadratic in λ with the solution

$$\lambda_0 = 1 - \frac{N}{2Y} - \sqrt{\left(\frac{N}{2Y}\right)^2 + \frac{Ns}{Y}} \tag{34}$$

where the negative square root is chosen to give the correct sign for λ_0. The bounds on the probability of detection are

$$P_d\left(N,s,Y\right) \le C_B\left(N,s,Y,\lambda_0\right) \text{ for } Y > s+N \text{ } (\lambda_0 \text{ is positive}) \tag{35}$$

and

$$P_d\left(N,s,Y\right) \ge 1 - C_B\left(N,s,Y,\lambda_0\right) \text{ for } Y < s+N \text{ } (\lambda_0 \text{ is negative}). \tag{36}$$

The Chernoff bound C_B is calculated for each set of parameter values. If it is less than ε, the probability of detection is set to 0 for $Y > s + N$, or 1 for $Y < s + N$.

The probability of detection for a fluctuating target in noise is

$$\begin{aligned} P_d(N,s,Y,k) &= \int_Y^\infty \int_0^\infty P_T(s \mid S,k) P_R(\mu \mid s,N) ds\, d\mu \\ &= \int_Y^\infty \int_0^\infty \frac{s^{k-1}}{\Gamma(k)}\left(\frac{k}{S}\right)^k e^{-ks/S}\left(\frac{\mu}{s}\right)^{(N-1)/2} e^{-(\mu+s)} I_{N-1}\left(2\sqrt{\mu s}\right) ds\, d\mu \\ &= \int_Y^\infty \frac{e^{-\mu}\mu^{N-1}}{\Gamma(N)}\left(1+Ns/k\right)^{-k} {}_1F_1\left(k;N;\frac{\mu}{1+k/Ns}\right) d\mu \end{aligned} \tag{37}$$

where ${}_1F_1(a;c;z)$ is the confluent hypergeometric function [4, §9.210/1]. This result was obtained by Swerling [8, equation (54)]. It also appears as equation (9) in reference [5], but the latter version contains several typographical errors.

The Chernoff bound for this case is

$$\begin{aligned} C_B(N,s,Y,k,\lambda) &= \int_0^\infty e^{\lambda(\mu-Y)} \frac{e^{-\mu}\mu^{N-1}}{\Gamma(N)}\left(1+Ns/k\right)^{-k} {}_1F_1\left(k;N;\frac{\mu}{1+k/Ns}\right)d\mu \\ &= \frac{e^{-\lambda Y}}{\Gamma(N)}\left(1+Ns/k\right)^{-k}\int_0^\infty e^{-\mu(1-\lambda)}\mu^{N-1}\,{}_1F_1\left(k;N;\frac{\mu}{1+k/Ns}\right)d\mu \qquad (38) \\ &= \frac{e^{-\lambda Y}}{(1-\lambda)^N}\left(1-\frac{Ns}{k}\frac{\lambda}{1-\lambda}\right)^{-k}. \end{aligned}$$

Equation (38) is evaluated using a definite integral of the confluent hypergeometric function [4, §7.621/5]:

$$\int_0^\infty t^{c-1}\,{}_1F_1(a;c;t)e^{-st}dt = \Gamma(c)s^{-c}\left(1-1/s\right)^{-a} \qquad (39)$$

The value of λ which gives the closest bound is obtained by solving

$$\frac{d\ln(C_B)}{d\lambda} = -Y + \frac{Ns}{(1-\lambda)^2}\left(1-\frac{Ns}{k}\frac{\lambda}{1-\lambda}\right)^{-1} + \frac{N}{1-\lambda} = 0 \qquad (40)$$

for λ. Equation (40) can be rearranged to form a quadratic in λ with the solution

$$\lambda_0 = b/2 - \sqrt{b^2/4 - c} \qquad (41)$$

where

$$\begin{aligned} b &= 1 - \frac{N}{Y} + \frac{1}{1+Ns/k}, \\ c &= \frac{1-N(1+s)/Y}{1+Ns/k}. \end{aligned} \qquad (42)$$

Appendix C: Interpolation Scheme

In a calculation of radar performance as a function of ground range, the signal to noise ratio, the clutter to noise ratio and the grazing angle all vary from point to point. The clutter shape parameter ν also changes, because it depends on the grazing angle. Thus the nodes and weights for the integration over the clutter power, which depend on ν, must be recalculated at every point. This makes the calculation method described here rather slow for calculations of radar performance such as those in [22]. It may be preferable to tabulate the probability of detection as a function of signal to interference ratio (*SIR*) [4] for different values of ν, and then use interpolation in this table for the radar performance calculation.

The probability of detection table has three variable parameters: *SIR*, *CNR* and ν. Variations in many parameters of interest, such as sea surface wind speed and direction, and platform altitude, speed and heading, affect only these three variables. Other radar parameters such as the false alarm number and the number of pulses integrated remain constant, however if they are changed the table must be recalculated.

Linear interpolation is satisfactory if a logarithmic scale is used for the variable parameters, and it is convenient to use the built-in Matlab function for interpolation in three dimensions for this purpose. Instead of interpolating $\log(\nu)$, it may be advantageous to interpolate the quantity

$$\eta = \log_{10}\left(1+\tfrac{\nu_0}{\nu}\right) \tag{43}$$

The *SIR* for $P_d = 0.5$ is approximately linear in η (Figure 12), and the Rayleigh case ($\nu \to \infty$) corresponds to $\eta = 0$, which enables interpolation between this case and finite values of ν. (The main effect of varying ν is a shift of the P_d curve to higher signal to interference ratios as ν decreases, which is quantified by the *SIR* required for $P_d = 0.5$.) Watts and Wicks [2] use an empirical expression in the form (43) for the signal to clutter ratio for $P_d = 0.5$. In their expression ν_0 depends on the false alarm number and the target fluctuation model, but for the purposes of interpolation it is sufficient to use a constant. If we take $\nu_0 = 9.9$, η ranges from 0 to 2 as ν varies from infinity down to 0.1.

[4] *SIR* = *SNR*/(1+*CNR*) in clutter and noise; *SIR* = *SCR* in clutter only.

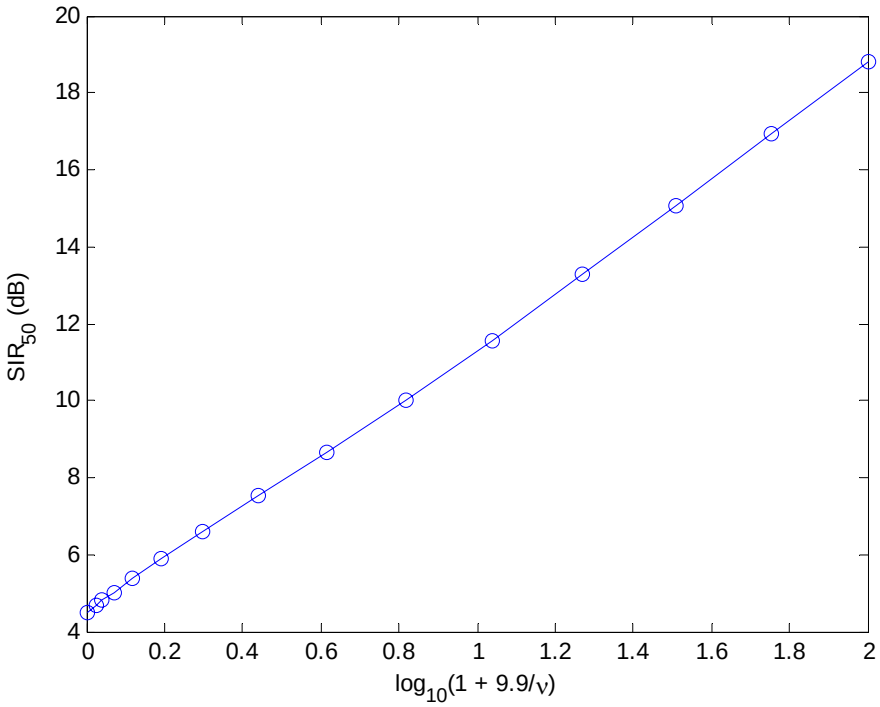

Figure 12 Signal to interference ratio for P_d = 0.5 plotted against the parameter η (equation (43)). This example is for the incoherent sum of 5 pulses from a Swerling 2 target in K-distributed clutter, with a probability of false alarm of 10^{-4}.

The effect of *CNR* on the P_d curve is highly non-linear. It also depends on ν: if ν is small, varying *CNR* has a significant effect, whereas if ν is large the clutter is noise-like so varying *CNR* has little effect (Figure 13). The dependence on ν makes it difficult to linearise the effect of *CNR*, but the quantity

$$\xi = \log_{10}\left(1+\frac{9}{1+\frac{1}{CNR}}\right) \tag{44}$$

is useful for interpolation. As *CNR* varies from 0 to ∞, ξ ranges from 0 to 1.

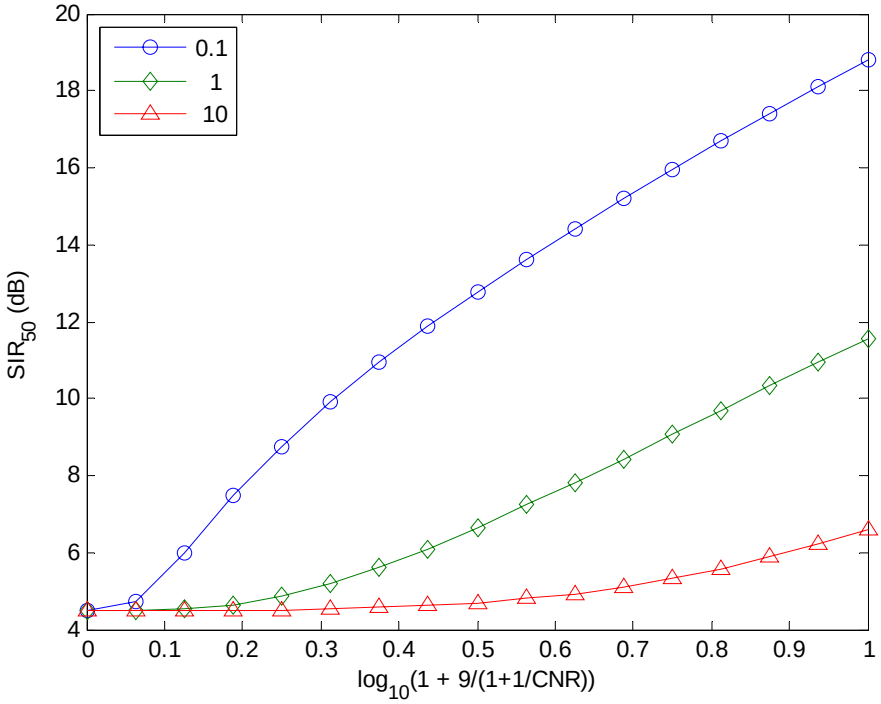

Figure 13 Signal to interference ratio for P_d = 0.5 plotted against the parameter ξ (equation (44)), for different values of the clutter shape parameter ν. This example is for the incoherent sum of 5 pulses from a Swerling 2 target in K-distributed clutter, with a probability of false alarm of 10^{-4}.

Steps of 0.5 dB in *SIR*, steps of 0.125 in η, and steps of 0.0625 in ξ were found to be sufficient to create a table for successful interpolation of the probability of detection for fluctuating targets. The interpolation table contained a total of 81×17×17 = 23409 points, with *SIR* ranging from -5 dB to 35 dB. Many points in the interpolation table lie outside the Chernoff bounds (Appendix B), and P_d is set to 0 or 1 without calculation at these points. The nodes and weights for integration only need to be calculated once for each value of ν in the table, and the detection threshold only needs to be calculated once for each combination of ν and *CNR*. Preparation of the table in this way took 3.7 s, compared with 50.7 s to calculate the same set of P_d values individually, with the nodes and weights for integration and the detection threshold computed separately for every point [5]. Clearly interpolation is only worthwhile if creating the interpolation table takes less time than direct calculation of P_d at the required points. The Matlab interpolation functions are much more efficient if the entire matrix of required data points is interpolated with a single function call, rather than interpolating the points one by one in a nested loop. Interpolation of 23120 points took 0.01 s with a single function call.

[5] Calculations carried out with Matlab R2010a on a 32 bit desktop computer with a 2.66 GHz quad core Pentium processor, running Windows XP.

The P_d curves for fixed targets can be very steep, so a finer grid is needed for successful interpolation; steps of 0.1 dB in *SIR*, steps of 0.1 in η, and steps of 0.0625 in ξ were used, for a total of 401×21×17 = 143157 points. Computation of this larger table took 12.3 s (306 s with the nodes and weights for integration and the detection threshold computed separately for every value of P_d).

The number of variables for interpolation can be reduced to two if ν is replaced by

$$\nu_{eff} = \nu\left(1+\tfrac{1}{CNR}\right)^2 \tag{45}$$

In this case the calculation is done for clutter only, so the probability of detection is tabulated as a function of *SCR* and η, with ν replaced by ν_{eff} in equation (43). Equation (45) is derived in Appendix D. This approximation is satisfactory for a clutter to noise ratio of ~10 dB or greater, or for any *CNR* if ν is ~10 or greater. It does not work so well for spiky clutter (small ν) and low *CNR* [1, Section 9.3.3.1].

Appendix D: Effective Shape Parameter

The effective shape parameter ν_{eff} for the clutter plus noise distribution is obtained by matching the normalised second intensity moment of the combined distribution to that of the K distribution for clutter alone [21]. The first two moments of the clutter plus noise distribution are ([1], p113 with $b = \nu/p_c$):

$$\left\langle z \right\rangle_{cn} = p_c + p_n \tag{46}$$

$$\left\langle z^2 \right\rangle_{cn} = 2p_c^2\left(1+\tfrac{1}{\nu}\right) + 4p_c p_n + 2p_n^2 \tag{47}$$

For the clutter only distribution we have

$$\left\langle z \right\rangle_{c} = p_c \tag{48}$$

$$\left\langle z^2 \right\rangle_{c} = 2p_c^2\left(1+\tfrac{1}{\nu}\right) \tag{49}$$

The normalised second intensity moment is

$$\frac{\left\langle z^2 \right\rangle_c}{\left\langle z \right\rangle_c^2} = 2\left(1+\tfrac{1}{\nu}\right) \tag{50}$$

Hence

$$\nu = \frac{2\left\langle z \right\rangle_c^2}{\left\langle z^2 \right\rangle_c - 2\left\langle z \right\rangle_c^2} \tag{51}$$

For the clutter plus noise distribution we have, making use of equations (46) and (47),

$$\begin{aligned} \nu_{eff} &= \frac{2\left\langle z \right\rangle_{cn}^2}{\left\langle z^2 \right\rangle_{cn} - 2\left\langle z \right\rangle_{cn}^2} \\ &= \frac{2\left(p_c + p_n\right)^2}{2p_c^2\left(1+\tfrac{1}{\nu}\right) + 4p_c p_n + 2p_n^2 - 2p_c^2 - 4p_c p_n - 2p_n^2} \\ &= \frac{\left(1+\tfrac{1}{CNR}\right)^2}{1+\tfrac{1}{\nu}-1} \\ &= \nu\left(1+\tfrac{1}{CNR}\right)^2 \end{aligned} \tag{52}$$

DISTRIBUTION LIST

Calculation of Radar Probability of Detection in K-Distributed Sea Clutter and Noise

Stephen Bocquet

AUSTRALIA

DEFENCE ORGANISATION	**No. of copies**
Task Sponsor	
DGAD	1 Printed
S&T Program	
Chief Defence Scientist Chief, Projects and Requirements Division DG Science Strategy and Policy	Doc Data Sht & Exec Summary (Shared)
Counsellor Defence Science, London	Doc Data Sheet
Counsellor Defence Science, Washington	Doc Data Sheet
Scientific Adviser to MRDC, Thailand	Doc Data Sheet
Scientific Adviser Intelligence and Information	1
Navy Scientific Adviser	Doc Data Sht & Dist List
Scientific Adviser – Army	Doc Data Sht & Dist List
Air Force Scientific Adviser	1
Scientific Adviser to the DMO	Doc Data Sht & Dist List
Scientific Adviser – VCDF	Doc Data Sht & Dist List
Scientific Adviser – CJOPS	Doc Data Sht & Dist List
Scientific Adviser – Strategy	Doc Data Sht & Dist List
Deputy Chief Defence Scientist Platform and Human Systems	Doc Data Sht & Exec Summary
Chief of Joint Operations Division	Doc Data Sht & Dist List
Research Leader Future Operations	Doc Data Sht & Dist List
Head Joint Systems Analysis (JOD)	1
Head Tactical Air Operations (AOD)	1
Science Team Leader: Martin Cross (AOD)	1
Author: Stephen Bocquet	1 Printed
Doug Driscoll (AOD)	1
Josef Zuk (AOD)	1
Brett Haywood (EWRD)	1

Yunhan Dong (EWRD)	1
Daniel Finch (EWRD)	1
David Crisp (ISRD)	1
Luke Rosenberg (ISRD)	1
DSTO Library and Archives	
Library Fishermans Bend	Doc Data Sheet
Library Edinburgh	1 Printed
Capability Development Group	
Director General Maritime Development	Doc Data Sheet
Director NCW Development	Doc Data Sheet
Assistant Secretary Investment Analysis	Doc Data Sheet
Chief Information Officer Group	
DICTF	Doc Data Sheet
Strategy Executive	
Policy Officer, Counter-Terrorism and Domestic Security	Doc Data Sheet
Vice Chief of the Defence Force Group	
SO (Science) - Counter Improvised Explosive Device Task Force	Doc Data Sht & Exec Summary & Dist List
Joint Logistics Command	
Directorate of Ordnance Safety	1
Head Engineering Systems	
Director General Strategic Logistics	Doc Data Sheet
Military Strategic Commitments	
Director General Military Strategic Commitments	Doc Data Sheet
Navy	
Maritime Operational Analysis Centre, Building 89/90 Garden Island Sydney NSW	Doc Data Sht & Dist List
Deputy Director (Operations)	
Deputy Director (Analysis)	
Director General Navy Capability Plans & Engagement	Doc Data Sheet
Director General Navy Communications & Information Warfare	Doc Data Sheet
Director General Navy Certification and Safety	Doc Data Sheet
Head Navy Engineering	Doc Data Sheet
Commodore Training	Doc Data Sheet
Commander Surface Force	Doc Data Sheet
Commander Mine Warfare, Clearance Diving, Hydrographic, Meteorological and Patrol Force	Doc Data Sheet
Commander Fleet Air Arm	Doc Data Sheet
Commander Submarine Force	Doc Data Sheet
Commodore Flotillas	Doc Data Sheet
Commodore Support	Doc Data Sheet
SO Science Fleet Headquarters	1

Army

Australian National Coordination Officer ABCA (AS NCO ABCA), Land Warfare Development Centre, Puckapunyal	Doc Data Sht
SO(Science) Forces Command	1
SO (Science) - Special Operations Command (SOCOMD) Russell Offices Canberra	Doc Data Sht & Exec Summary & Dist List
SO(Science) 1st Division	Doc Data Sheet
SO2 S&T FDG LWDC - (Staff Officer for Science and Technology, Force Development Group)	Doc Data Sheet
SO(Science) 1Bde	Doc Data Sheet
SO(Science) 3Bde	Doc Data Sheet
SO(Science) 17 CSS Bde	Doc Data Sheet
J86 (TCS GROUP), DJFHQ	Doc Data Sheet

Air Force

SO (Science) - Headquarters Air Combat Group, RAAF Base, Williamtown NSW 2314	Doc Data Sht & Exec Summary
Staff Officer Science Surveillance and Response Group	Doc Data Sht & Exec Summary
SO (Science) Combat Support Group	Doc Data Sht & Exec Summary
Staff Officer Science HQ Air Lift Group	Doc Data Sht, Exec Summary & Dist List

Intelligence and Security Group

AS Transnational and Scientific Intelligence, DIO	Doc Data Sheet
Manager, Information Centre, Defence Intelligence Organisation	1
Director Advanced Capabilities, DIGO	Doc Data Sheet

Defence Materiel Organisation

CoS GM Systems	Doc Data Sheet
Program Manager Air Warfare Destroyer	Doc Data Sheet
Guided Weapon & Explosive Ordnance Branch (GWEO)	Doc Data Sheet
Director Engineering Operations; Land Engineering Agency (Michael Yates)	Doc Data Sheet
CSIO	Doc Data Sheet
Deputy Director Joint Fuel & Lubricants Agency	Doc Data Sheet
Systems Engineering Manager CBRNE Program Office, Land Systems Division	Doc Data Sheet

OTHER ORGANISATIONS

National Library of Australia	1
NASA (Canberra)	1

UNIVERSITIES AND COLLEGES

Australian Defence Force Academy

Library	1
Head of Aerospace and Mechanical Engineering	1
Hargrave Library, Monash University	Doc Data Sheet

OUTSIDE AUSTRALIA

INTERNATIONAL DEFENCE INFORMATION CENTRES

US Defense Technical Information Center	1
UK Dstl Knowledge Services	1
Canada Defence Research Directorate R&D Knowledge & Information Management (DRDKIM)	1
NZ Defence Information Centre	1

ABSTRACTING AND INFORMATION ORGANISATIONS

Library, Chemical Abstracts Reference Service	1
Engineering Societies Library, US	1
Materials Information, Cambridge Scientific Abstracts, US	1
Documents Librarian, The Center for Research Libraries, US	1
International Technology and Science Center (ITSC) Library	1

INFORMATION EXCHANGE AGREEMENT PARTNERS

National Aerospace Laboratory, Japan	1
National Aerospace Laboratory, Netherlands	1

SPARES	4 Printed

Total number of copies: 37 Printed: 6 PDF: 31

*In keeping with the DSTO Research Library's *Policy on Electronic distribution of official series reports,* unclassified, xxx-in confidence and restricted reports will be sent to recipients via DRN email as per the distribution list. Authors, task sponsors, libraries and archives will continue to receive hard copies.

DEFENCE SCIENCE AND TECHNOLOGY ORGANISATION
DOCUMENT CONTROL DATA

1. PRIVACY MARKING/CAVEAT (OF DOCUMENT)

2. TITLE

Calculation of Radar Probability of Detection in K Distributed Sea Clutter and Noise

3. SECURITY CLASSIFICATION (FOR UNCLASSIFIED REPORTS THAT ARE LIMITED RELEASE USE (L) NEXT TO DOCUMENT CLASSIFICATION)

Document	(U)
Title	(U)
Abstract	(U)

4. AUTHOR(S)

Stephen Bocquet

5. CORPORATE AUTHOR

DSTO Defence Science and Technology Organisation
Fairbairn Business Park Department of Defence
Canberra ACT 2600 Australia

6a. DSTO NUMBER	6b. AR NUMBER	6c. TYPE OF REPORT	7. DOCUMENT DATE
DSTO-TN-1000	AR-014-977	Technical Note	April 2011

8. FILE NUMBER	9. TASK NUMBER	10. TASK SPONSOR	11. NO. OF PAGES	12. NO. OF REFERENCES
2011/1022353	CDE07/040	DGAD	26	22

13. DSTO Publications Repository

http://dspace.dsto.defence.gov.au/dspace/

14. RELEASE AUTHORITY

Chief, Joint Operations Division

15. SECONDARY RELEASE STATEMENT OF THIS DOCUMENT

Approved for public release

OVERSEAS ENQUIRIES OUTSIDE STATED LIMITATIONS SHOULD BE REFERRED THROUGH DOCUMENT EXCHANGE, PO BOX 1500, EDINBURGH, SA 5111

16. DELIBERATE ANNOUNCEMENT

No Limitations

17. CITATION IN OTHER DOCUMENTS Yes

18. DSTO RESEARCH LIBRARY THESAURUS http://web-vic.dsto.defence.gov.au/workareas/library/resources/dsto_thesaurus.shtml

Radar detection; Sea clutter; Mathematical analysis

19. ABSTRACT

The detection performance of maritime radars is usually limited by sea clutter. The K-distribution is a well established statistical model of sea clutter which is widely used in performance calculations. There is no closed form solution for the probability of detection in K-distributed clutter, so numerical methods are required. The K-distribution is a compound model which consists of Gaussian speckle modulated by a slowly varying mean level, this local mean being gamma distributed. A series solution for the probability of detection in Gaussian noise is integrated over the gamma distribution for the local clutter power. Gauss-Laguerre quadrature is used for the integration, with the nodes and weights calculated using matrix methods, so that a general purpose numerical integration routine is not required. The method is implemented in Matlab and compared with an approximate solution based on lookup tables. The solution described here is slower, but more accurate and more flexible in that it allows for a wider range of target fluctuation models.